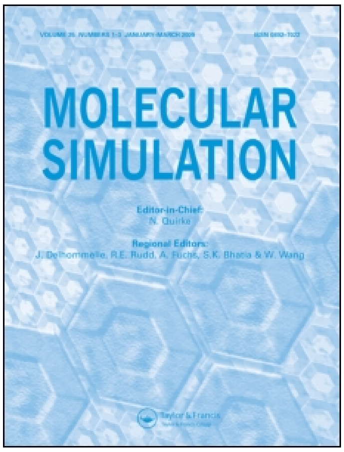

Molecular Simulation
Publication details, including instructions for authors and subscription information:
http://www.informaworld.com/smpp/title~content=t713644482

Molecular Dynamics and Hypernetted Chain Equation Studies of Soft Core Repulsions in Electrolyte Solutions

Lianrui Zhang[a]; M. Jinno[ab]; H. Ted Davis[a]; Henry S. White[a]
[a] Department of Chemical Engineering and Materials Science, University of Minnesota, Minneapolis, MN [b] Mitsubishi Heavy Industries, Ltd., Minatoku, Nagoya, Japan

To cite this Article Zhang, Lianrui , Jinno, M. , Davis, H. Ted and White, Henry S.(1994) 'Molecular Dynamics and Hypernetted Chain Equation Studies of Soft Core Repulsions in Electrolyte Solutions', Molecular Simulation, 12: 1, 1 — 21

To link to this Article: DOI: 10.1080/08927029408022532

URL: http://dx.doi.org/10.1080/08927029408022532

Molecular Simulation, 1994, Vol. 12(1), pp. 1-21
Reprints available directly from the publisher
Photocopying permitted by license only

MOLECULAR DYNAMICS AND HYPERNETTED CHAIN EQUATION STUDIES OF SOFT CORE REPULSIONS IN ELECTROLYTE SOLUTIONS

LIANRUI ZHANG, M. JINNO[(a)], H. TED DAVIS, and HENRY S. WHITE

Department of Chemical Engineering and Materials Science, University of Minnesota, Minneapolis, MN 55455

(Received February 1993, accepted July 1993)

Effects of the repulsive soft core pair potential $r^{-\nu}$ in 1:1 electrolytes (1 molar concentration) are studied by molecular dynamics (MD) simulations and by the hypernetted chain (HNC) integral equations. Comparisons on the electrolyte structure and dynamical properties are made between a (a) soft ion (SI) model and a (b) soft ion in solution (SIS) model of electrolyte. In the SI model, there is no solvent, whereas the SIS model has ions and neutral solvent molecules at liquid density. Inclusion of the solvent imparts liquid-like structure to the ion-ion pair correlation functions and, if $\nu \neq \infty$, gives rise to substantial back scattering oscillations in the velocity autocorrelation functions with a consequent reduction in the particle self diffusion coefficient. Larger values of ν reduce the back scattering in the velocity autocorrelation functions. The dynamical behavior of the ions in the SI model is similar to that of the primitive model electrolyte ($\theta = \infty$) when $\nu \geqslant 9$. In the SIS fluid, all the pair correlation functions have a similar oscillatory structure with roughly the same first peak separation for every pair. Simulation results obtained with the minimum image method compare well with those obtained with the more expensive Ewald sum method. The HNC theory predicts pair correlation functions in good agreement with simulations of fluids with continuous repulsive forces but over-predicts pair correlations in hard sphere fluids.

KEY WORDS: Electrolyte solutions, soft core repulsion, HNC equation, molecular dynamics simulations

I INTRODUCTION

The primitive model electrolyte, a fluid of charged hard spheres with a dielectric constant ε, has been a popular model for computer simulations aimed at developing and testing theories of molecular structure in electrolyte solutions and electrical double layers [1-6]. The hypernetted chain (HNC) approximation and variations of it have been quite successful for the primitive model electrolyte [7-12]. There are, of course, numerous differences between a real electrolyte and the primitive model electrolyte. These differences include the presence of a neutral solvent, the existence of continuous forces instead of hard sphere repulsion, a nonspherical structure of the solvent molecules, and the existence of multipolar and polarization forces among the molecules. There have been many simulations of water and ionic solutions [13-18] using more or less realistic atomic structure and intermolecular forces. However, the theory of such systems has not kept pace with simulations because of the complexities

---

(a) Permanent Address: Mitsubishi Heavy Industries, Ltd., 10 Oye-cho, Minatoku, Nagoya 455, Japan.

of polyatomic fluids. We thus feel that there is still some value in carrying out molecular simulations on simplified models that go beyond the primitive electrolyte model and reflect some of the molecular factors of a real system but that remain more amenable to theoretical analysis than would be a fully realistic model.

We report here a study of a electrolyte model in which a solvent is present and whose particles interact with continuous repulsive forces rather than hard sphere forces. We retain in the model the assumptions that the molecular forces are spherically symmetric and that the polar forces can be accounted for by a dielectric constant. The purposes of the work are to (1) compare the primitive model (PM) electrolyte with a model electrolyte having solvent molecules, (2) study the effect of stiffness or steepness of continuous short range forces on the equilibrium and dynamical properties of the electrolyte with and without solvent molecules, (3) compare the results of simulations using the Ewald sum [19] method with the results of simulations using the less expensive minimum image method, and (4) compare simulation results with HNC theory.

In particular, we report in what follows the effects of choosing different inverse power law intermolecular repulsions $1/r^{-\nu}$ (with $\nu = 4,6,9,12,24$, and ∞) and of the absence or presence of solvent molecules in two model systems of 1:1 electrolytes: (a) one is a modified version of the primitive model electrolyte in which all ions are soft spheres instead of hard spheres and the solvent is represented by a dielectric constant ε; (b) the other in which the ions and solvent molecules are represented by soft spheres instead of hard spheres and the polar interactions are represented by a dielectric constant ε. We shall call case (a) the soft ion (SI) model electrolyte and case (b) the soft ion in solution (SIS) model electrolyte.

II MODEL SYSTEM

The systems investigated are bulk 1:1 electrolytes comprised of either (a) soft sphere ions or (b) soft sphere ions and soft sphere neutral solvent molecules. The unit cell for the simulation is a cubic box of size $L \times L \times L$ which contains N particles of (a) the SI model electrolyte or (b) the SIS model electrolyte. The system consists of the unit cell and its periodic extension in three dimensions. All the simulations reported here were carried out at a bulk concentration of $C = 1$ molar and a temperature of $T = 298.16\,\text{K}$. The interactions between particles inside the boxes are composed of two parts: the core repulsion between all particles and the Coulomb interaction between ions. The interactions between particles i and j for systems (a) and (b) are chosen to be of the form

$$u(r_{ij}) = u_\nu^R(r_{ij}) + \frac{q_i q_j}{\varepsilon r_{ij}}, \tag{2.1}$$

where the repulsive potential is

$$u_\nu^R(r) = B_\nu (d/r)^\nu \tag{2.2}$$

Here d represents the size parameter of the ions and solvent molecules, q_i the molecular charge of species i (value times the electronic charge), and d, ν, and B_ν parameters of the repulsive interactions. ε is the dielectric constant (chosen to be 78.5, the value of bulk liquid water). Only eq.(2.2) is used for ion-solvent and solvent-

solvent interactions. The coefficient B_ν is chosen such that it will satisfy equation (2.1), for a close-packed electrically neutral sodium chloride crystal structure with $\varepsilon = 1$. Thus, B_ν is given by the relation [7,9,20]

$$B_\nu = \frac{A_m |q_+ q_-|}{N_c \nu d}. \tag{2.3}$$

where A_m, Madelung's constant, and N_c, the coordination number, are equal to 1.74 and 6 for this crystal. For a 1:1 electrolyte, this gives $B_\nu = 6.68 \times 10^{-20}/\nu d$ in units of erg·cm. The power ν determines how fast the core repulsion decays, i.e., it determines the range of the repulsive interaction. For finite ν, an effective ionic diameter can be estimated from the first peak in the unlike-ion pair crorrelation functions and is always larger than d. In the limit of infinite ν, d is the hard core diameter.

For long range potentials and forces, the Ewald summation is the technique that often used in simulations in summing the Coulomb fields. The formula for the potential has two parts. One is the real space sum which is a double summation and the other is a reciprocal space sum and can be written as a single summation,

$$U(r) = \sum_{\mathbf{R}} \frac{1}{|\mathbf{R} + \mathbf{r}|} = \frac{2\pi}{V_c} \sum_{G} \frac{e^{-G^2/4G_0^2}}{G^2} e^{i\mathbf{G}\cdot\mathbf{r}} + \sum_{\mathbf{R}} \frac{\operatorname{erfc}(G_0 |\mathbf{R} + \mathbf{r}|)}{|\mathbf{R} + \mathbf{r}|}. \tag{2.4}$$

R and **G** are the real and reciprocal space lattice vectors respectively. The summation over the ion indices i and j has been omitted in eq.(2.4). The second term contains the complementary error function erfc(x),

$$\operatorname{erfc}(x) \equiv 1 - \operatorname{erf}(x) = \frac{2}{\sqrt{\pi}} \int_x^\infty dz e^{-z^2}, \tag{2.5}$$

which goes to zero rapidly at large values of its argument x. The self energy term gives a contribution of

$$U_s = \sum_i^N q_i^2 \frac{G_0}{\sqrt{\pi}}, \tag{2.6}$$

and is subtracted from equation (2.4).

The procedure for using this technique is to choose a value of G_0 which makes both the real and reciprocal space series converge faster than the origin series in (2.4). We try to avoid the summations over the real space lattice vectors which require double loops in the simulations. The complementary error function which goes to 10^{-4} as its argument goes to 3. The value of G_0 that is used in the simulation is $5/L$ which gives an accuracy of 10^{-4}.

III SIMULATIONS

Molecular dynamics simulations are based on tracking the motions of particles determined by Newtons's law. For continuous potentials, the integrations of the particle trajectory are performed using a simple scheme of first obtaining the velocity

$$\mathbf{v}(t + \Delta t) = \mathbf{v}(t) + \mathbf{a}(t)\Delta t, \tag{3.1}$$

and then advancing the particle position

$$\mathbf{r}(t+\Delta t) = \mathbf{r}(t) + \mathbf{v}(t)\Delta t. \qquad (3.2)$$

$\mathbf{v}(t)$ is the velocity, $\mathbf{a}(t) = \mathbf{F}/m$ is the acceleration at time t and Δt is the time step.

For hard sphere systems, the collision dynamics of the system must be solved on a collision by collision basis [21]. In the primitive model electrolyte, we have both hard sphere core and the Coulomb potential outside the core. In this case, a hybrid molecular dynamics method is used [4,5]. We briefly describe the procedures here.

The step by step approach of the MD program can be described in the following: (i) Calculate the force and advance the particle positions according to eqs.(3.1-2). (ii) If the particles overlap in the configurations created in step (i), then (iii) determine the collision time t_{ij} between the particles i and j,

$$|\mathbf{r}_{ij}(t+t_{ij})| = |\mathbf{r}_{ij} + \mathbf{v}_{ij}t_{ij}| = d \qquad (3.3)$$

where $\mathbf{r}_{ij} = \mathbf{r}_i - \mathbf{r}_j$ and $\mathbf{v}_{ij} = \mathbf{v}_i - \mathbf{v}_j$. Let us define $b_{ij} = \mathbf{r}_{ij} \cdot \mathbf{v}_{ij}$, then

$$v_{ij}^2\, t_{ij}^2 + 2t_{ij}\, b_{ij} + r_{ij}^2 - d^2 = 0. \qquad (3.4)$$

(a) If $b_{ij} > 0$, the two particles are receding and no collision will occur. (b) If $b_{ij} < 0$, then, if $b_{ij}^2 - v_{ij}^2 \cdot (r_{ij}^2 - d^2) < 0$, the equation has complex roots and no collision will occur. Otherwise, the smallest collision time can be determined by

$$t_{ij} = \frac{-b_{ij} - \sqrt{b_{ij}^2 - v_{ij}^2(r_{ij}^2 - d^2)}}{v_{ij}^2}. \qquad (3.5)$$

Step (iv) is to find the shortest collision time t_{ij} and advance particle positions during this time. (v) The particle velocities are computed after the collision and (vi) a search for the next collision (steps (iii) - (v)) is begun until the configuration is fully resolved.

The structural properties of a liquid are measured by the pair correlation functions $g_{\alpha\beta}(r)$. The function $g_{\alpha\beta}$ is defined as the probability of finding a pair of particles α and β a distance r apart, relative to the probability expected for a completely random distribution function at the same density (the positive, negative, and neutral species are denoted by $\alpha, \beta = +, -, 0$). The dynamical properties are represented by the velocity autocorrelation functions $C_\alpha(t)$. Self diffusion coefficients can be calculated from the mean square displacements or from velocity autocorrelation functions.

The mean square displacement of particles of species α is defined by

$$R_\alpha^2(t) = \frac{1}{N_\alpha}\sum_{i=1}^{N_\alpha} \langle |\mathbf{r}_i(t+t_0) - \mathbf{r}_i(t_0)|^2 \rangle, \quad \alpha = +, -, 0 \qquad (3.6)$$

where $\langle \cdots \rangle$ denotes an average over different time origins t_0, i.e., different initial times. N_α is the number of particles of species α. The velocity autocorrelation function is defined by,

$$C_\alpha(t) = \frac{\sum_{i=1}^{N_\alpha} \langle \mathbf{v}_i(t+t_0) \cdot \mathbf{v}_i(t_0) \rangle}{\sum_{i=1}^{N_\alpha} \langle \mathbf{v}_i(t_0)^2 \rangle}, \quad \alpha = +, -, 0 \qquad (3.7)$$

where the notations have the same meanings as in eq (3.6). $\mathbf{v}_i(t + t_0)$ is the particle velocity at time $t + t_0$ and $\mathbf{v}_i(t_0)$ is the particle velocity at the time origin t_0.

The mean square displacement consists of two time regimes. The first regime is the short time regime, in which $R_\alpha^2(t)$ increases nonlinearly with time; the second regime is one in which $R_\alpha^2(t)$ increases linearly and in which the particle diffusivity can be obtained from the Einstein relation

$$D_\alpha = \lim_{t \to \infty} R_\alpha^2(t)/6t. \tag{3.8}$$

The diffusion coefficients can also be computed from the velocity autocorrelation functions, via

$$D_\alpha = \frac{1}{3N_\alpha} \sum_{i=1}^{N_\alpha} \int_0^\infty \langle \mathbf{v}_i(t + t_0) \cdot \mathbf{v}_i(t_0) \rangle \, dt. \tag{3.9}$$

Diffusion coefficients calculated from the two approaches are slightly different as will be seen in the simulation results reported below. This is due to the small number of particles and the finite simulation times.

The mean potential energy $\langle u \rangle$ is computed from the formula

$$\langle u \rangle = \frac{1}{2} \sum_{i,j} \langle u(r_{ij}) \rangle. \tag{3.10}$$

IV HNC THEORY FOR ELECTROLYTES

For a bulk electrolyte with ion and solvent molecules at number densities n_k, $k = 0, +, -$, the Ornstein-Zernike (OZ) equation is

$$h_{ij}(r_{12}) = c_{ij}(r_{12}) + \sum_k n_k \int c_{ik}(r_{13}) h_{kj}(r_{32}) d^3 r_3 \tag{4.1}$$

where $c_{ij}(r_{12})$ and $h_{ij}(r_{12}) = g_{ij}(r_{12}) - 1$ are the direct and total pair correlation functions. In the hypernetted chain (HNC) approximation

$$h(r) = c(r) + \ln g(r) + u(r)/k_B T \tag{4.2}$$

where k_B is the Boltzmann constant and T is the temperature. Equation (4.1) can be written as [22]

$$\begin{aligned} \ln y_{ij}(r_{12}) = \sum_k n_k \int & [f(r_{13}) y(r_{13}) + y(r_{13}) - 1 \\ & - \ln y(r_{13})]_{ik} [(h(r_{32}) + 1) y(r_{32}) - 1]_{kj} d^3 r_3 \end{aligned} \tag{4.3}$$

with

$$g(r) = y(r)\,(f(r) + 1). \tag{4.4}$$

The volume element $d^3 r_3$ was expressed in bipolar coordinates, namely,

$$d^3 r_3 = \frac{2\pi}{r_{12}} r_{13} r_{23} dr_{13} dr_{23}, \tag{4.5}$$

in solving Eq(4.3).

Table I Comparisons of the results obtained from the soft ion (SI) model electrolytes of $\nu = 9,12$, and ∞ by using the minimum image method and Ewald sum technique in the molecular dynamics simulations for the 1:1 electrolyte, with an ion diameter $d = 2.8428$ Å. The cubic unit cell has a side length of 56.39 Å and the simulation temperature is 298.16 Kelvin. The unit cell contains 108 cations and 108 anions with a molar mass of 18. The dielectric constant is taken to be 78.5. The unit used in this table for D is 10^{-3} cm^2/s.

ν	*Method*	D_+		D_-		$\langle u\rangle/NkT$	*Nsteps*
		R_α^2	C_α	R_α^2	C_α		(10^4)
9	MI	3.898	3.913	3.768	3.756	−0.5227	8.0
12		4.009	4.026	4.011	4.028	−0.5714	8.0
∞		3.881	3.861	3.970	4.002	−0.6641	8.0
9	Ewald	3.868	3.845	3.915	3.928	−0.5217	4.0
12		4.124	4.167	4.046	4.040	−0.5715	4.0
∞		3.940	3.980	4.050	4.030	−0.6618	4.0

Using the Newton Raphson method with an initial guess for y(r), we found that Eq.(4.3) usually can be solved within 10 iterations and an error

$$\Delta = \sqrt{\sum_i |y_{i+1} - y_i|^2} \leqslant 10^{-7}.$$

for the SI model. For the SIS model, the solutions obtained for low density electrolytes were used as initial guesses for continuation of Newton Raphson iteration to higher density solutions. Using this strategy, a few more iterations are required to obtain a similar level of accuracy for the SIS model.

V RESULTS

A *The soft ion (SI) model electrolyte*

The molecular dynamics simulations were carried out with the aid of the algorithm given in Section III. For the SI model electrolyte, there was a total of 216 ions in the cubic box, the length of its side was 56.39 Å. During the simulation, an initial 6000 steps were used to equilibrate the system, and then another 4 to 16×10^4 steps were used to accumulate averages of positions and velocities for later analysis. The time step used was $\Delta t = 10^{-14}$ seconds and the ions were assigned the same characteristic length $d = 2.84$ Å and same molar mass of 18. Values of $\nu = 4,6,12,24$, and ∞ were chosen in different simulations of this system.

The minimum image (MI) method has been shown to be quite accurate in simulations of primitive model electrolytes. From figures 1 to 3, we can see that the minimum image method works well for the soft ion model electrolyte in comparison to the results obtained by using the Ewald summation. The pair correlation functions of the two methods agree well over most of the range, although appreciable deviations occur near the main peak of the pair correlation functions as ν becomes smaller. Simulations by the two methods are in good agreement for the mean potential energy, mean square displacement, velocity autocorrelation functions and diffusivities as is demonstrated by Figures 1-3 and Table I. We also see in Figures 1-3 that the pair correlation functions obtained from HNC integral equations are in nearly perfect agreement with the simulation results obtained using Ewald summation. Using several

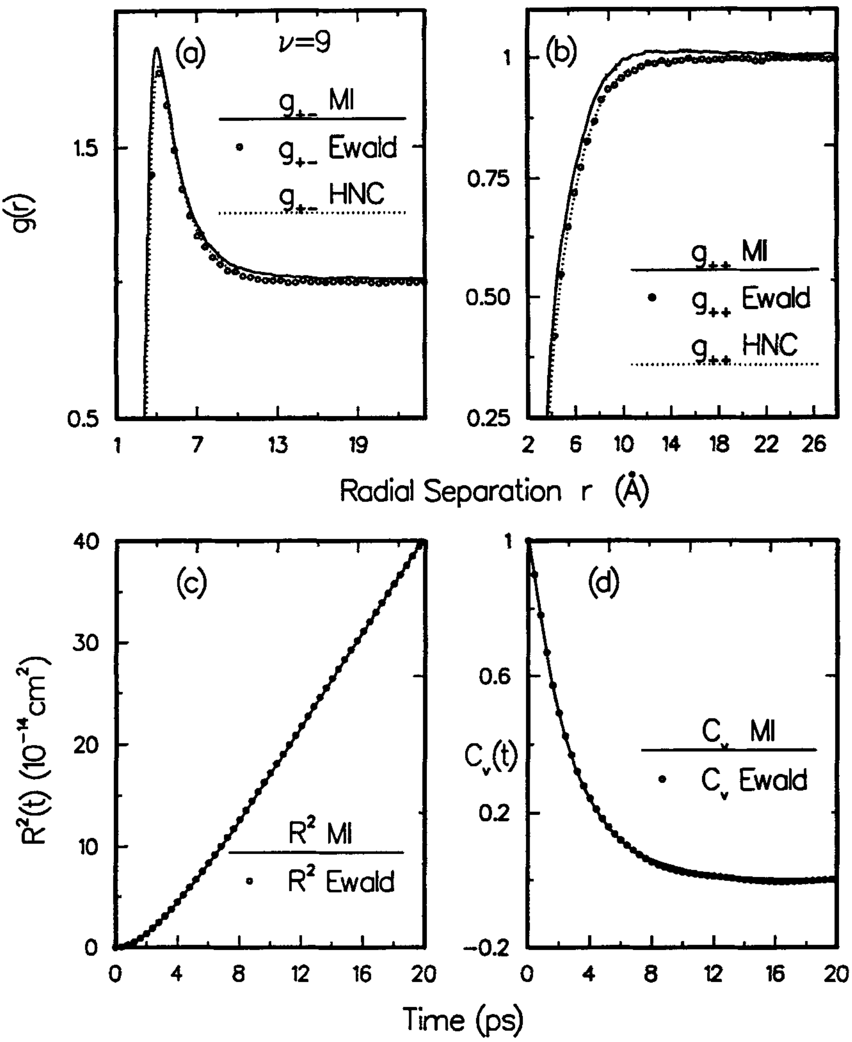

Figure 1 Comparisons of the unlike-ion pair correlation functions for a soft ion (SI) model 1:1 electrolyte with $\nu = 9$ at a concentration of 1 molar. Ion size parameter $d = 2.84$ Å. Keys: $N = 216$ using Ewald, (—); Minimum image (MI), (o); *HNC*, (· · ·).

simulation segments which have the same number of time steps, the errors of the pair correlation functions, the mean square displacements, and the velocity autocorrelation functions were estimated. The computed errors, plotted in figures 1-3, are less than or comparable to the width of lines used to plot the results, and are very small compared with the differences between the results obtained from MI and Ewald sum.

With increasing steepness of the core repulsion (i.e., increasing ν), the nearest neighbor peak of the unlike-ion pair correlation function $g_{+-}(r)$ increases in

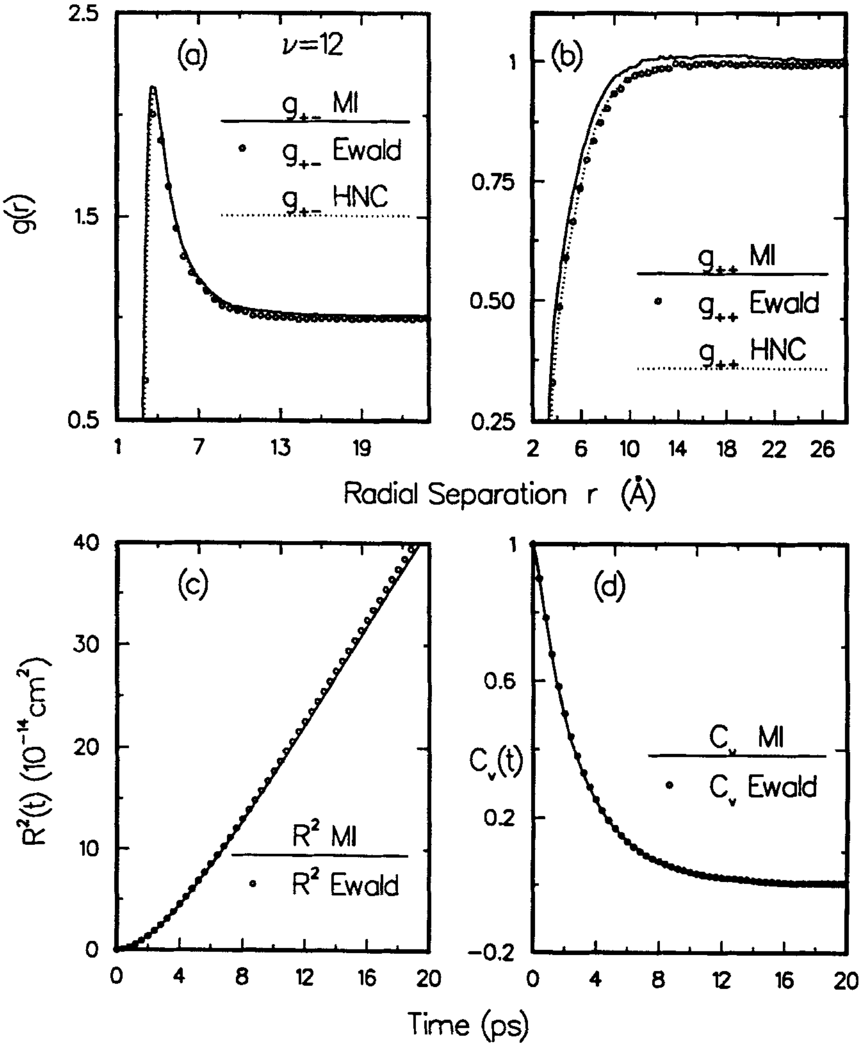

Figure 2 Comparisons of the unlike-ion pair correlation functions for a soft ion (SI) model 1:1 electrolyte with $\nu = 12$ at a concentration of 1 molar. Ion size parameter $d = 2.84$ Å. Keys: $N = 216$ using Ewald, (—); Minimum image (MI), (o); *HNC*, (···). The vertical bars represent the deviations of the simulation. You can barely notice them at the peak of the like-ion pair correlation function.

magnitude and shifts to smaller separation values (see figure 4). Similarly, the distance of closest approach of the like- and unlike-ions, i.e., the separation at which $g_{\alpha\beta} \approx 0$, decreases towards the hard sphere diameter as ν increases (figures 4a and 4b). These results show the importance of the non-ionic core repulsion in determining the ionic structure.

In figures 4c and 4d, the mean square displacements and velocity autocorrelation functions are given for different values of ν. The mean square displacements are linear

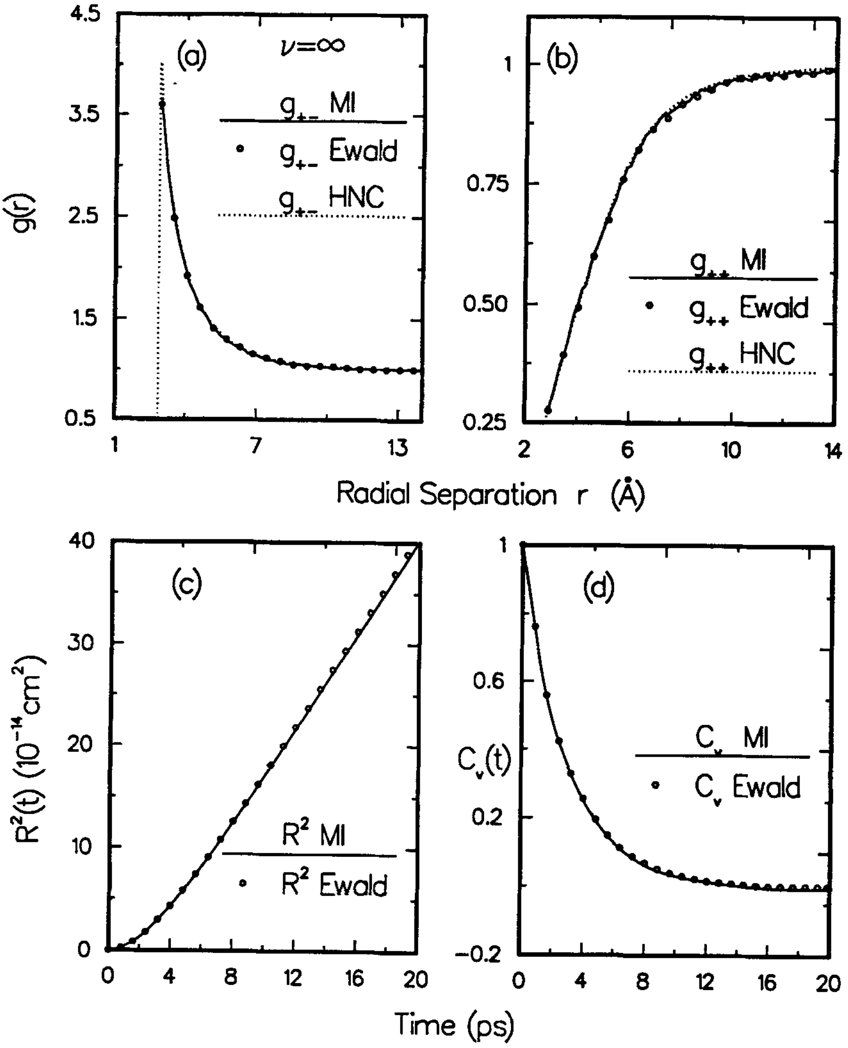

Figure 3 Comparisons of the unlike-ion pair correlation functions for a soft ion (SI) model 1:1 electrolyte with $\nu = \infty$ at a concentration of 1 molar. Ion size parameter $d = 2.84$ Å. Keys: $N = 216$ using Ewald, (−); Minimum image (MI), (o); *HNC*, (···).

functions of time for times greater than 5 to 7×10^{-12} seconds. Diffusion coefficients calculated from the linear regions as a function of ν are shown in figure 5. The errors due to limited number of particles and finite simulation time may be the causes of the differences between D_+ and D_- and between the values of D_α obtained from eqs (3.3) and (3.4). The values of D_+ and D_- obtained from the primitive model electrolyte ($\nu = \infty$) simulations are given in Table I. It is evident from fig. 5 that a stronger core repulsion (larger ν) results in a larger ion self diffusion coefficient. This dependence on ν is qualitatively similar to the diffusivity predicted

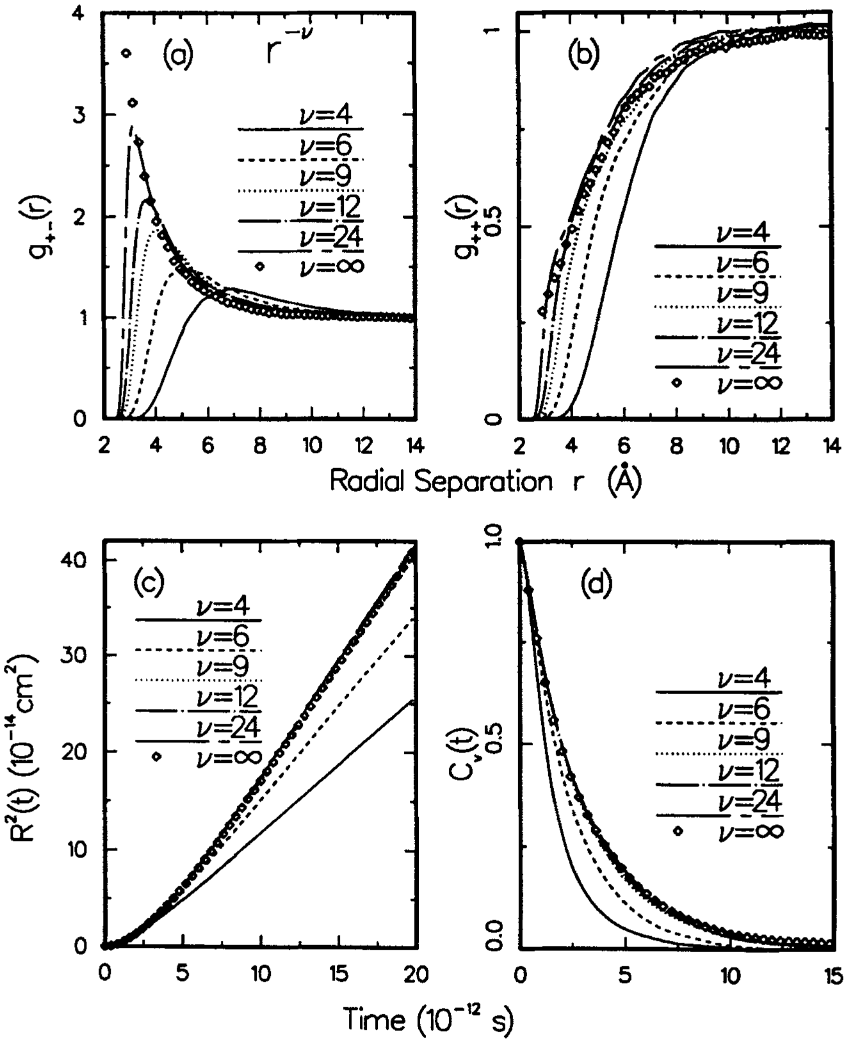

Figure 4 (a) Unlike- and (b) like-ion pair correlation functions from simulations for six different ν values of 4, 6, 9, 12, 24, and ∞ (hard sphere) in the SI model. (c) Mean square displacements, and (d) velocity autocorrelation functions as a function of time.

by dilute gas theory of diffusion in a soft sphere fluid [23]. The behavior results from the fact that the scattering cross section increases with the range of the repulsive potential and the range increases with decreasing ν. It follows from figures 4–6 that the dynamical behavior of the particles with $\nu \geqslant 9$ is quite similar to that of hard sphere particles.

As a measure of the effective range of a repulsive pair potential, Barker and Henderson [21] proposed the following formula for the effective hard core diameter d_e of a pair of molecules interacting via the repulsive pair potential $u_\nu^R(r)$:

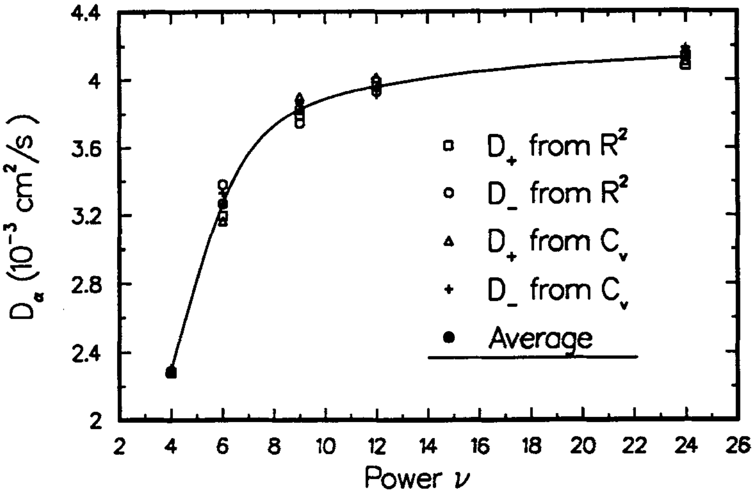

Figure 5 Ion self-diffusion coefficients as a function of the power ν of the inverse repulsion potential in the SI model.

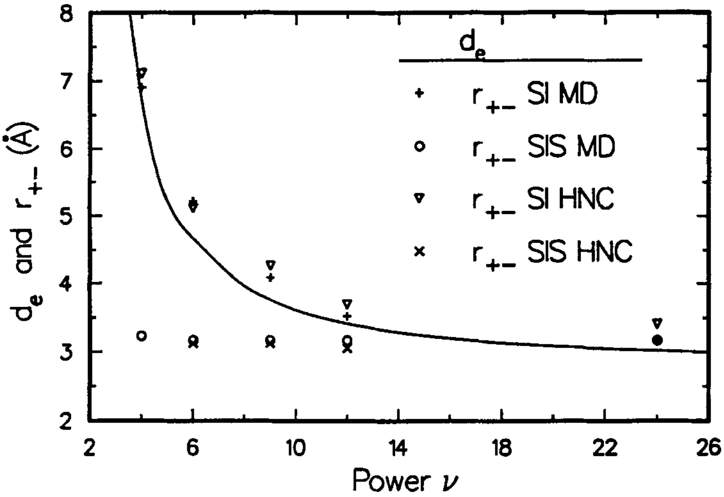

Figure 6 Effective particle diameter d_e calculated from the Barker-Henderson approximation and the separation r_{+-} of the first peaks of the unlike-ion pair correlation functions in the SI and SIS model electrolytes as a function of the core repulsion power ν at room temperature.

$$d_e = \int_0^\infty [1 - \exp(-u_\nu^R(r)/k_B T)]\,dr. \tag{5.1}$$

Integration of eq (5.1) for different powers of repulsion ν in $u_\nu^R(r) = B_\nu(d/r)^\nu$ gives the dependence of d_e on the power ν. The results are compared in figure 6 to the positions of the first peaks (nearest peaks) of the unlike-ion pair distribution functions r_{+-} from simulations and HNC results as a function of ν. The fact that d_e and the

Table II Comparisons of the results obtained from the soft ion in solution (SIS) model electrolytes of $\nu = 6,9,12$, and ∞ by using the minimum image method and Ewald sum technique in the molecular dynamics simulations for the 1:1 electrolyte, with an ion diameter $d = 2.8428$ Å. The cubic unit cell has a side length of 25.51 Å and the simulation temperature is 298.16 Kelvin. The unit cell contains 10 cations, 10 anions, and 556 neutral solvent molecules for $\nu = 6,9$ and 12 and 12 cations, 12 anions, and 667 neutral solvent molecules for $\nu = \infty$. The molar mass of all the particles is 18 and the dielectric constant is taken to be 78.5. The unit used in this table for D is 10^{-5} cm^2/s.

ν	*Method*	D_+		D_-		D_0		$\langle u\rangle/NkT$		*Nsteps*
		R^2_α	C_α	R^2_α	C_α	R^2_α	C_α	*MD*	*HNC*	(10^5)
6	MI	2.389	2.429	2.303	2.305	2.349	2.365	24.056	25.079	6
9		2.183	2.159	2.295	2.291	2.263	2.246	9.310	10.171	4
12		2.752	2.758	2.707	2.650	2.729	2.721	4.926	5.625	3.2
6	Ewald	2.264	2.207	2.303	2.265	2.281	2.275	24.050		2
9		2.210	2.196	2.300	2.193	2.217	2.226	9.303		3
12		2.769	2.682	2.608	2.462	2.792	2.788	4.925		3
∞		6.873	6.962	6.764	6.748	6.906	6.977	−0.717		4

unlike-ion nearest neighbour separations are so close indicates that the short range forces contribute importantly to ionic packing in the SI model electrolyte. In the next section we shall see that the presence of a solvent removes much of the sensitivity of ionic structure to short range repulsive forces between ions.

B *The soft ion in solution (SIS) model electrolyte*

For the SIS model simulations, we examined 20 soft ions and 556 neutral soft solvent molecules inside a cubic unit cell, the length of whose sides is 25.51 Å. For simplicity, each ion and neutral solvent molecule was assumed to have the same characteristic length parameter, $d = 2.84$ Å, and the same molar mass, 18. This system is used to represent qualitatively a 1:1 electrolyte at a concentration of 1 molar and a temperature of 298.16 K with a bulk water density of $1 g/cm^3$. The particle number density is then roughly $n^* = nd^3 \sim 0.8$. The first 26000 steps were used to reach equilibrium and the following 2 to 6×10^5 steps to compute averages. In this part of the simulations, a smaller time step of $\Delta t = 2 \times 10^{-15}$ seconds was used to obtain a more accurate calculation of the velocity autocorrelation functions. Values of $\nu = 4,6,9,12$, and ∞ were used in modeling the core repulsion.

As can be seen from table II, the differences in the mean potential energy obtained using the Ewald sum and minimum image are less than 0.1%. The average diffusivities differ less than 10%. Figures 7 to 11 give the simulated pair distribution functions, mean square displacements, and velocity autocorrelation functions for $\nu = 6,9,12$, and ∞. In each figure, a comparison is made between results from the minimum image method shown as (MI) and Ewald sum shown as (Ewald). In this part, just as in the SI simulations shown in part **A**, the errors of our simulations are estimated by using several segments of simulations and are shown as vertical bars in figures 7 through 11. There is substantial error near the maxima in the pair correlation functions.

Graphs 7a-11a demonstrate that, unlike the situation for the solvent free electrolyte, the pair correlation function $g_{+-}(r)$ has a liquid-like oscillatory structure for all values of ν, in agreement with the HNC integral equation results shown in figures 12e-h. (For the purpose of comparison, the pair correlation functions obtained

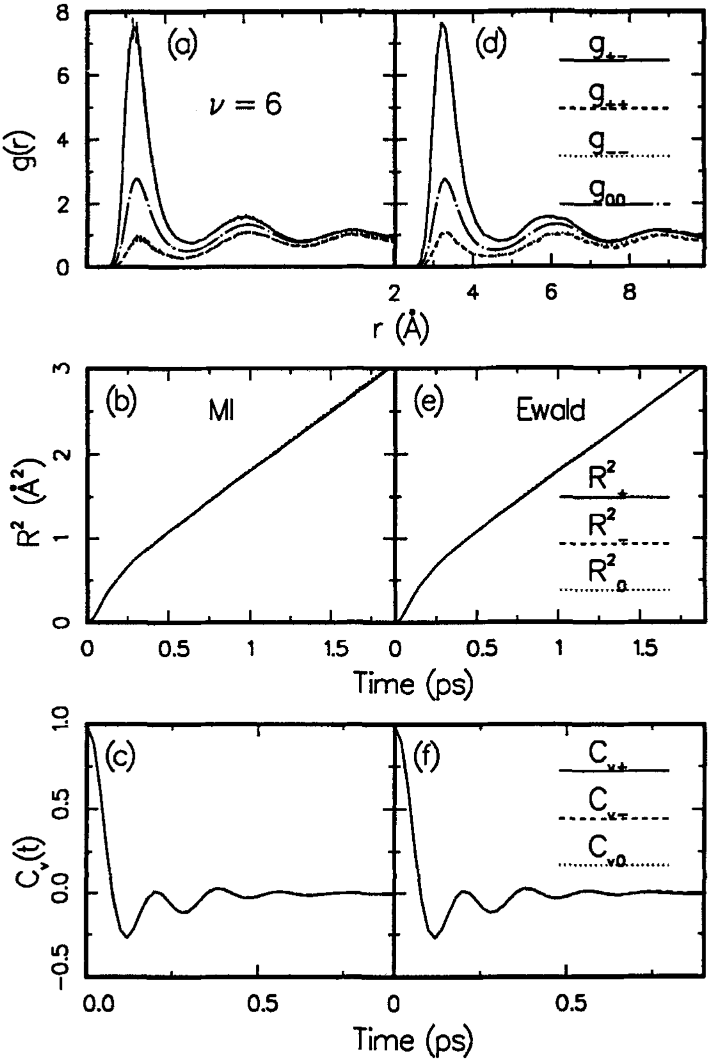

Figure 7 Comparisons of the simulation results between the minimum image method and the Ewald sum method: (a) Pair distribution functions for the core repulsion $\nu = 6$ in the SIS model. (b) Mean square displacements. (c) Velocity autocorrelation functions. The vertical bars represent the magnitude of the deviations.

from Ewald sum method were drawn again in Fig. 12). This oscillatory structure may at first appear strange since the density of the ions is low and is the same in both cases. However, this behavior can be understood in terms of a neutral multicomponent fluid of particles interacting with the same pair potential as in eq(2.2). Since the pair potential is the same for all the species, the pair correlation function $g_{\alpha\beta}(r)$ is the same for every pair $\alpha\beta$, i.e., $g_{\alpha\beta}(r) = g(r)$, where $g(r)$ is the pair correlation function of a pure fluid at the same total number density, $n = \Sigma_\alpha n_\alpha$, of the mixture.

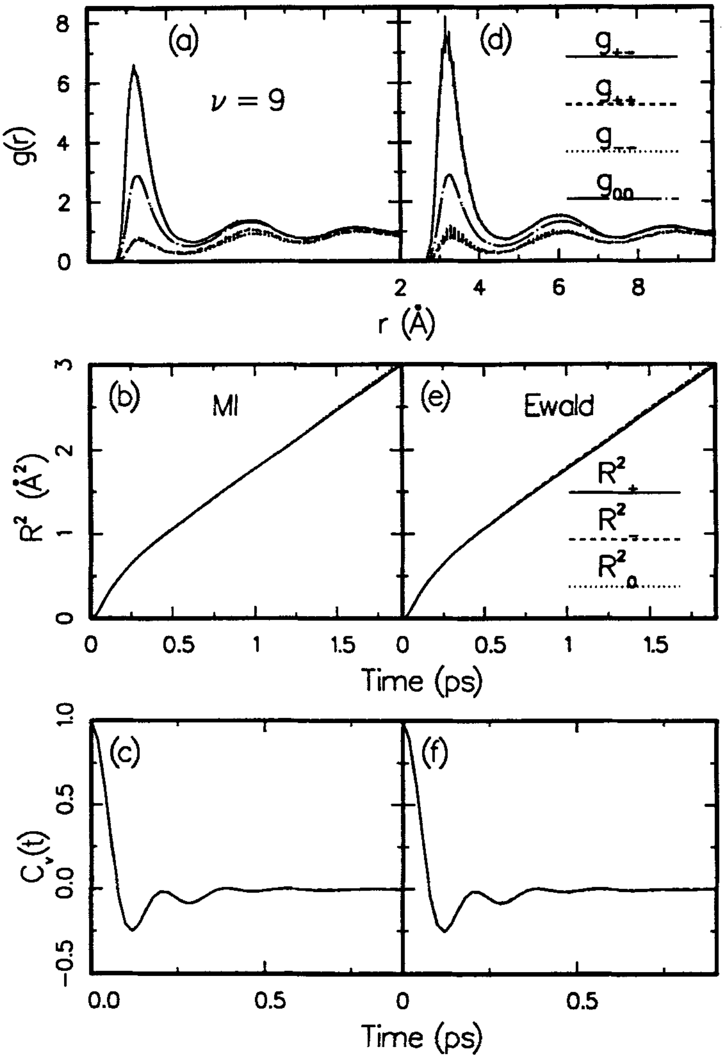

Figure 8 Same as figure 7 using $\nu = 9$ in the SIS model.

It is known that in a dense fluid, the short-range repulsive force plays a major role in controlling fluid structure. Thus it is reasonable to expect the pair correlation function for our model to be of the form [24]

$$g_{\alpha\beta}(r) = g^R(r)e^{w_{\alpha\beta}(r)/k_BT}, \tag{5.2}$$

where $g^R(r)$ is the correlation function in a pure fluid of neutral particles whose pair potentials are given by eq (2.2), which is determined by the potential of mean force (PMF) [24]. $w_{\alpha\beta}(r)$ is a monotonically varying perturbation to the potential of mean force. Here, $w_{\alpha\beta}(r)$ arises from the Coulomb interaction. We expect that

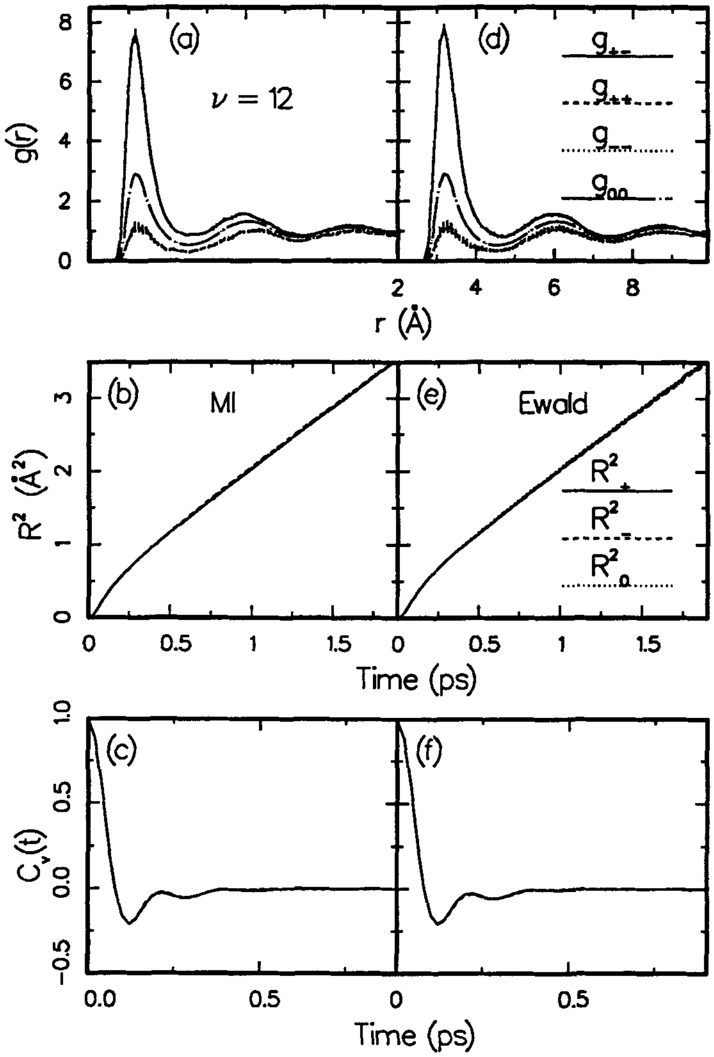

Figure 9 Same as figure 7 using $\nu = 12$ in the SIS model.

roughly $|w_{+-}| \approx |w_{++}| = |w_{--}|$ and $|w_{0+}| \approx |w_{0-}| \approx |w_{00}| \approx 0$ at the nearest neighbour peak. For $\nu = 12$, shown in figure 9a, we estimate $w_{\alpha\beta}(r_{peak})/k_B T \approx 0.97$ the maximum values of g_{+-} and g_{++} using Eq(5.2) and the assumption that $|w_{+-}| = |w_{++}|$. Under the above stated assumptions, we expect

$$g_{+-}^{max} \approx g_{00}^{max}\, e^{0.97} \text{ and } g_{++}^{max} \approx g_{00}^{max}\, e^{-0.97}. \tag{5.3}$$

Equation (5.3), with the aid of the observed value of $g_{00}^{max} = 2.9$, predicts $g_{+-}^{max} \approx 7.7$ and $g_{++}^{max} = 1.1$, which compare well with the observed values $g_{+-}^{max} = 7.8$ and $g_{++}^{max} = 1.1$.

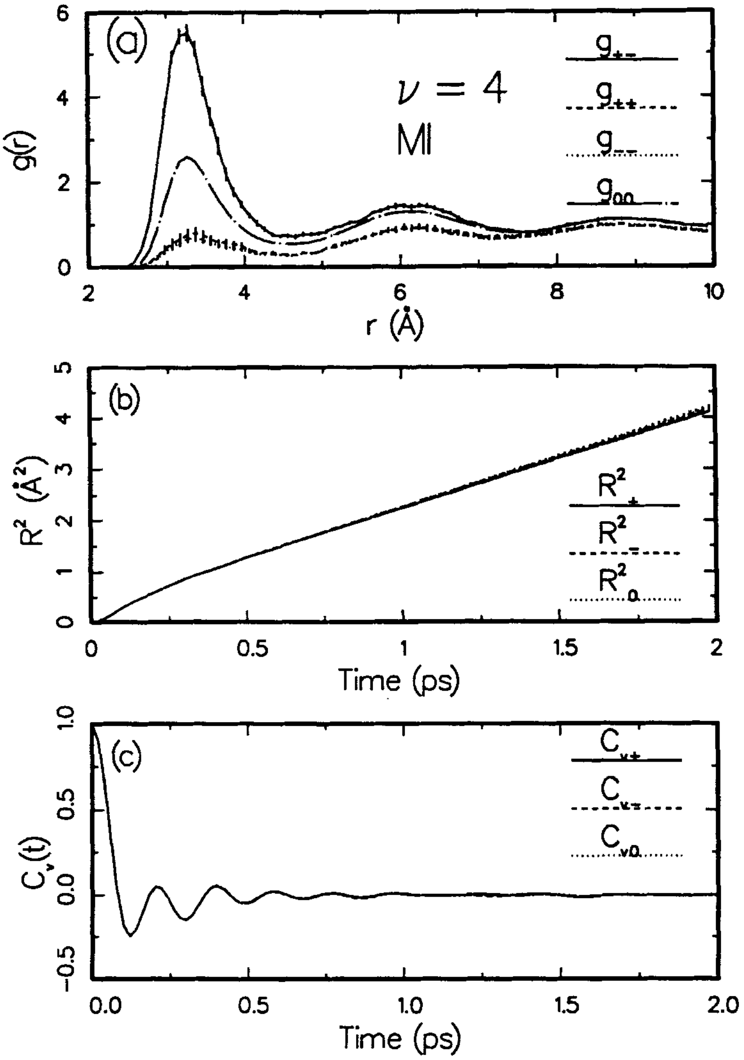

Figure 10 (a) Pair distribution functions for the core repulsion $\nu = 4$ in the SIS model. (b) Mean square displacements. (c) Velocity autocorrelation functions. The conditions of the simulation is the same as in figure 7.

Another implication of the argument given here is that g_{0+} and g_{0-} are approximately equal to g_{00}. Although we do not present all the results for $g_{0\alpha}(r)$, $\alpha = +,-$, we did compute these functions in both simulations and HNC theory and found them to be almost identical to $g_{00}(r)$ for all values of ν. With larger values of ν, the peak values of $g_{00}(r)$ increases slightly as can be seen from pair correlation functions shown in figures 7 to 12. This demonstrates that for a steeper core repulsion, the electrolyte is more structured owing to the more rigid *packing* requirement.

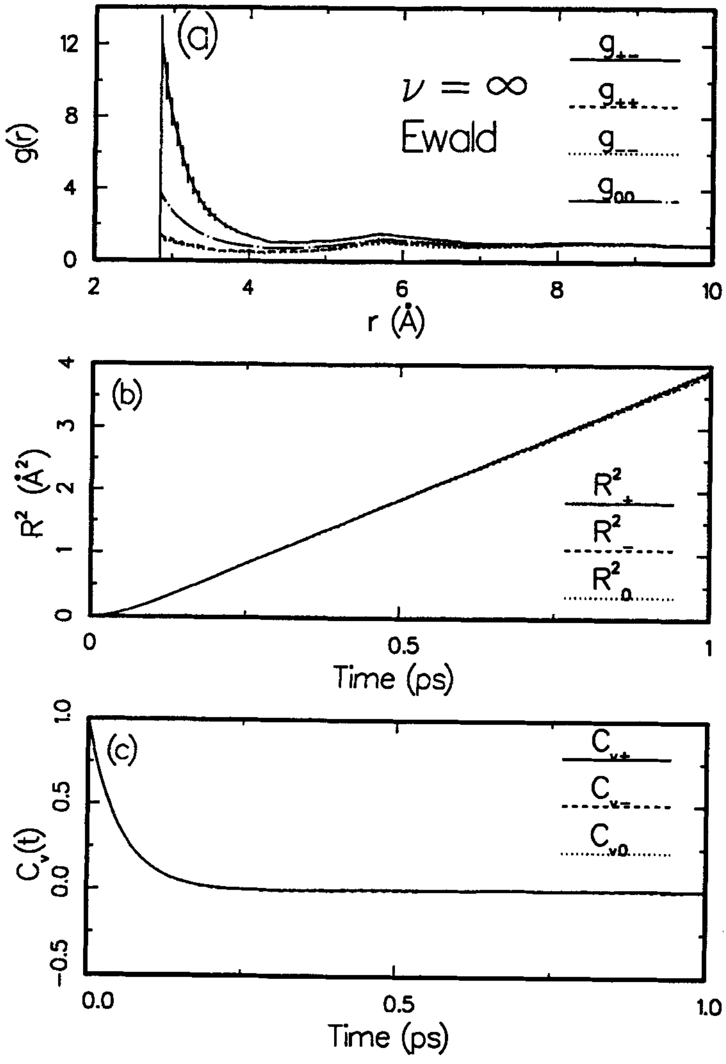

Figure 11 (a) Pair distribution functions for the hard sphere core repulsion ($\nu = \infty$) in SIS electrolyte. (b) Mean square displacements. (c) Velocity autocorrelation functions.

To appreciate qualitatively why the pair correlation function is so similar for all $\alpha\beta$ in a dense fluid no matter how small the densities of α and β are, consider again the case of particles obeying the same pair potential. Suppose $n^\alpha_\beta(r)$ denotes the probable density of species β at a distance r from the center of a particle of species α. By definition, the pair correlation function $g_{\alpha\beta}$ is related to $n^\alpha_\beta(r)$ by the expression $n^\alpha_\beta(r) = n_\beta g_{\alpha\beta}(r)$. Since interactions between the particles are the same for all species, the probable particle density at distance r from the center of a molecule of species α is $ng(r)$, where $n = \Sigma_\alpha n_\alpha$ and g(r) is the pair correlation function in a pure fluid of density n. n^α_β is then the product of $ng(r)$ and the probability x_β that

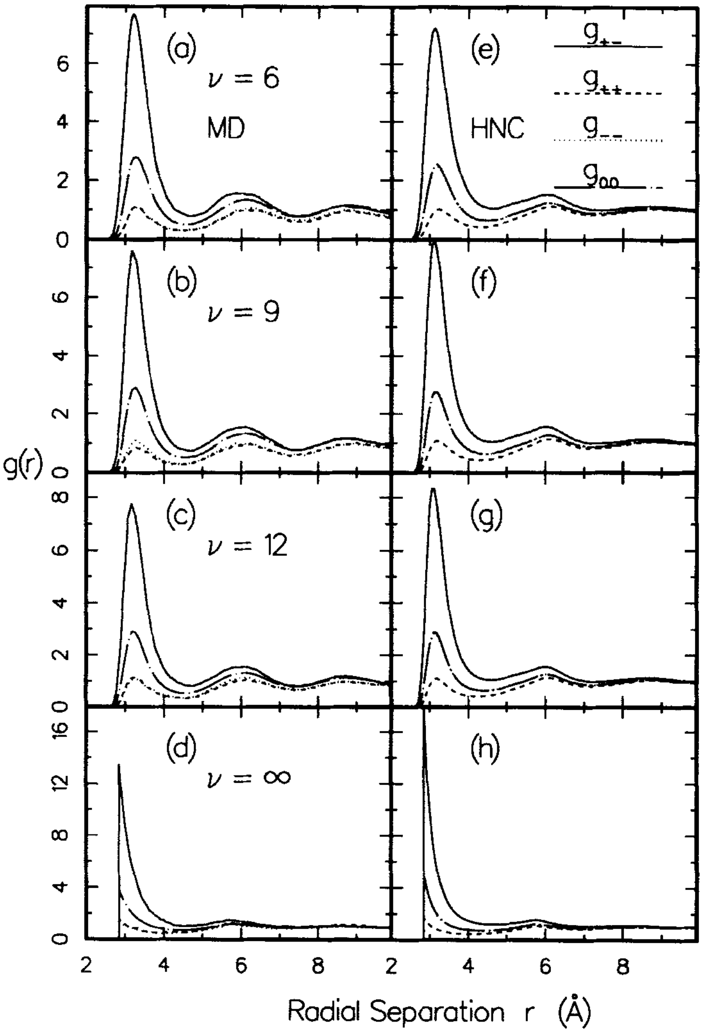

Figure 12 Comparisons of simulated pair distribution functions in SIS model with the results from HNC integral equation theory.

the particle at r is of species β, i.e., $n_\beta^\alpha(r) = x_\beta n g(r) = n_\beta g(r)$, or again we conclude that $g_{\alpha\beta}(r) = g(r)$ and is independent of $\alpha\beta$. x_β is the the mole fraction of species β.

Unlike the case for the SI model electrolyte, the nearest neighbor separations (positions of the first peak of $g_{\alpha\beta}$ are almost independent of ν (see figure 6). This is perhaps because of the high density constraint ($n^* \sim 0.8$) controls the packing spacing more than does the range of the repulsive interactions. Both MD simulations and the HNC theory demonstrate this phenomenon, as in figure 12. The HNC theory agrees well with simulations for $\nu \leqslant 12$, although the main peak predicted by the

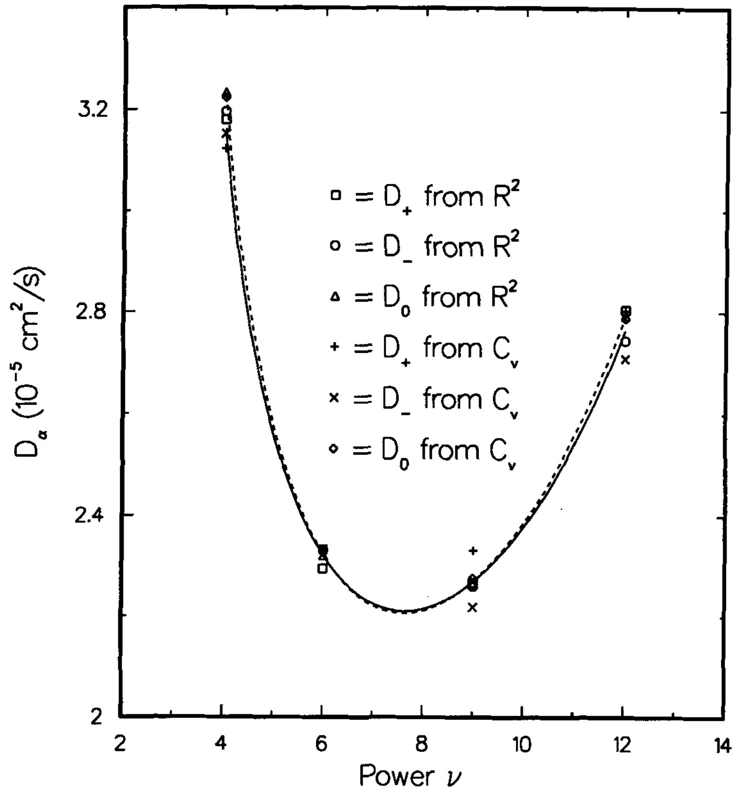

Figure 13 Ion and solvent molecule self-diffusion coefficients as a function of the power ν in the SIS model. The solid and dashed lines are the spline fit to the averages of solvent and ion (cation and anion) diffusion coefficients.

HNC theory is a few percent different from the simulation results. In the hard sphere limit $\nu = \infty$ the HNC theory seriously over-predicts the main peak in the pair correlation functions.

Figures 7–11b & c show the mean square displacements and the velocity autocorrelation functions of the ions and solvent molecules. Significant solvent effects are revealed once again in the oscillations of the correlation functions. The velocity autocorrelation functions of ions and solvent molecules are the same within the scatter of the simulations. As seen in figures 7c–11c, the oscillations slowly diminish as ν become larger (and the repulsive interactions becomes shorter ranged) and totally disappear for the hard sphere case. Thus, for the conditions studied here, there is significant back scattering in the case of continuous repulsive forces (e.g. $\nu \neq \infty$) and almost no back scattering occurs in the hard sphere limit ($\nu = \infty$). Back scattering does not occur in the SI model electrolyte because the density of scatterers is so low that only uncorrelated collisions occur.

The ion and solvent diffusivities computed from the simulated mean square displacements and velocity autocorrelation functions are plotted in figure 13. Unlike the results for the SI model electrolyte (figure 5), in which monotonically increasing diffusivities are observed with increasing ν, the diffusivities in the SIS model electrolyte have a minimum between $\nu = 7$ and 8. The diffusivities of the ions and solvent molecules are nearly the same. The diffusion coefficients obtained from a hard sphere simulation are given in table II. In the hard sphere simulation, we adopted a system of 12 cations and the Ewald sum method was used. At present, we cannot give a reason for the minimum in the D_α versus ν curve.

Acknowledgements

The Minnesota Supercomputer Institute (MSI), the National Science Foundation, and the Office of Naval Research provided support for this work.

References

[1] J.P. Valleau, L.K. Cohen, and D.N. Card, "Primitive model electrolytes. I. Grand canonical monte carlo simulations", *J. Chem. Phys.*, **72**, 5942 (1980); D.N. Card and J.P. Valleau, "Monte carlo study of the thermodynamics of Electrolyte solutions", *J. Chem. Phys.*, **52**, 6332 (1970).

[2] G.M. Torrie, and J.P. Valleau, "Electrical double layer. I. Monte carlo study of a uniformly charged surface", *J. Chem. Phys.*, **73**, 5807 (1980).

[3] L. Gulbrand, B. Jonsson, and H. Wennerstrom, "Electrical double layer forces. A monte carlo study", *J. Chem. Phys.*, **80**, 2221 (1985).

[4] D.M. Heyes, "Molecular dynamics simulations of restricted primitive model 1:1 electrolytes", *Chem. Phys.*, **69**, 155 (1982).

[5] S.H. Suh, L. Mier-y-Teran, H.S. White, and H.T. Davis, "Molecular dynamics study of the primitive model of 1:3 electrolyte solutions", *Chem. Phys.*, **142**, 203 (1990).

[6] L.R. Zhang, H.S. White, and H.T. Davis, "Simulation of confined electrolytes: application of a new method of summing the Coulomb field", *Mol. Simulation*, **9**, 247 (1992); Lianrui Zhang, H.T. Davis, and H.S. White, "Simulation of solvent effects on confined electrolytes", *J. Chem. Phys.*, **98**, 5793 (1993).

[7] J.C. Rasaiah and H.L. Friedman, "Integral equation methods in the computation of equilibrium properties of ionic solutions", *J. Chem. Phys.*, **48**, 2742 (1968); P. Rossky, J.B. Dudowicz, B.L. Tembe, and H.L. Friedman, "Ionic association in the model 2:2 electrolyte solutions", *J. Chem. Phys.*, **73**, 3372 (1980).

[8] A.R. Allnatt, "Integral equation in ionic solution theory", *Mol. Phys.*, **8**, 533 (1964).

[9] V. Vlachy, T. Ichiye, and A.D.J. Haymet, "Symmetric associating electrolytes: GCMC simulations and Integral equation theory", *J. Am. Chem. Soc.*, **113**, 1077 (1991); D.M. Duh and A.D.J. Haymet, "Integral equation theory for charged liquids: model 2-2 electrolytes and the bridge function", *J. Chem. Phys.*, **97**, 7716 (1992).

[10] E. Lomba and J.S. Hoye, "HNCR a program to calculate the structure and thermodynamics of binary mixtures of charged hard spheres", *Comp. Phys. Comm.*, **69**, 420 (1992).

[11] M. Kinoshita and M. Harada, "Numerical solution of the HNC equation for ionic systems", *Mol. Phys.*, **65**, 599 (1988).

[12] G.M. Abernethy and M.J. Gillan, "A new method of solving the HNC equation for ionic liquids", *Mol. Phys.*, **39**, 839 (1980).

[13] A. Rahman and F.H. Stillinger, "Molecular dynamics study of liquid water", *J. Chem. Phys.*, **55**, 3336 (1971); F.H. Stillinger and A. Rahman, "Molecular dynamics study of temperature effects on water structure and kinetics", *J. Chem. Phys.*, **57**, 1281 (1972).

[14] H.J.C. Berendsen, J.P.M. Postma, W.F. van Gunsteren, and J.H. ermans, "Interaction models of water in relation to protein hydration and kinetics", *Intermolecular forces*, edited by B, Pullman, (D. Reidel publishing company, 1981). p 331.

[15] G.N. Patey and G.M. Torrie, "Water and salt water near charged surfaces: a discussion of some recent theoretical results", *Chemica Scripta*, **29A**, 39 (1989).

[16] L.X. Deng, J.E. Rice, and P.A. Kollman, "The effect of water models on the interaction of the sodium-chloride ion pair in water: molecular dynamics simulations", *J. Chem. Phys.*, **93**, 2528 (1990).

[17] E. Guardia, R. Rey, and J.A. Padro, "Potential of mean force by constraint molecular dynamics: a sodium chloride ion-pair in water', *Chem. Phys.*, **155**, 187 (1991).

[18] D.E. Smith and A.J. Haymet, "Structure and dynamics of water and aqueous solutions: The role of flexibility", *J. Chem. Phys.*, **96**, 8450 (1992).

[19] P. Ewald, "Die Berechnung optischer und electrostatischer Gitterpotentiale", *Ann. Phys.*, **64**, 253 (1921); M.P. Allen and D.J. Tildesley, "*Computer Simulation of Liquids*", Clarendon Press, Oxford, 1987.

[20] L. Pauling, *The nature of the Chemical Bond*, (Cornell University Press), New York, 1960.

[21] B.J. Adler and T.E. Wainwright, "Studies in molecular dynamics I. General Method", *J. Chem. Phys.*, **31**, 459 (1959).

[22] J.A. Barker and D. Henderson, "What is 'liquid'? Understanding the state of matter", *Rev. Mod. Phys.*, **48**, 587 (1976).

[23] S. Chapman and T.G. Cowling, *The mathematical theory of nonuniform Gases*, Cambridge University Press, Cambridge, England, 1960.

[24] J.C. Rasaiah, "A view of electrolyte solutions", *J. Solut. Chem.*, **2**, 301 (1973).